Quark to Hadron Fragmentation Functions

Relation of BES-III Measurement to JLab-12 GeV SIDIS Experiments

Discussions at IHEP, Nov. 1st, 2013.

Xiaodong Jiang

Los Alamos National Laboratorv

- Spin independent Fragmentation Functions
- Spin dependent Fragmentation Functions

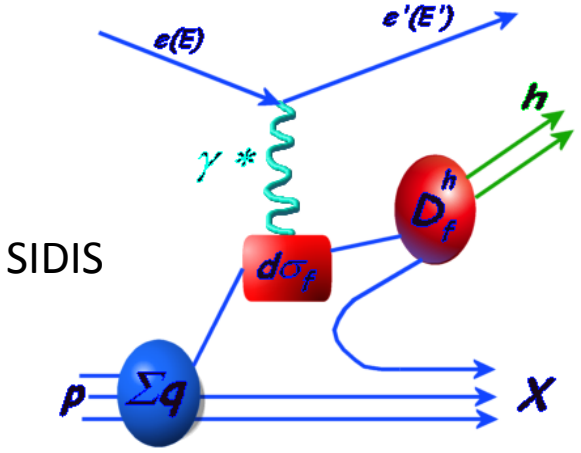

Universality ?
Vacuum vs inside a nucleaon ?

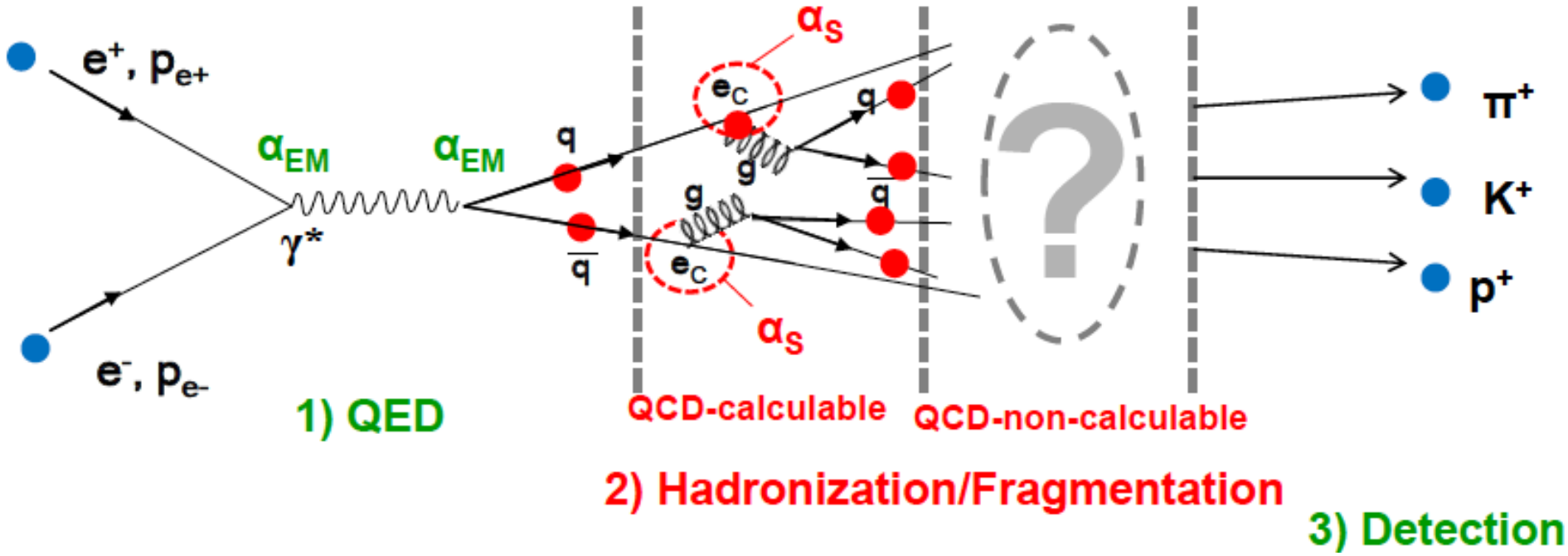

Four Types of Frag. Func.

- Spin independent Fragmentation Functions
- Spin dependent Fragmentation Functions
  (i.e. initial quark spin to final hadron azimuthal).
- Spin Transfer Fragmentation Functions
  (i.e. initial quark spin to final hadron spin)
- Fragmentation Function of Induced hadron polarization
  (i.e. unpolarized quark to polarized final hadron)

$$N^U(\phi) = \frac{\mathrm{d}\sigma(e^+e^- \to \pi^\pm\pi^\mp X)}{\mathrm{d}\Omega \mathrm{d}z_1 \mathrm{d}z_2} \propto \frac{5}{9} D^{\mathrm{fav}}(z_1)\overline{D}^{\mathrm{fav}}(z_2) + \frac{7}{9} D^{\mathrm{dis}}(z_1)\overline{D}^{\mathrm{dis}}(z_2)$$

$$N^L(\phi) = \frac{\mathrm{d}\sigma(e^+e^- \to \pi^\pm\pi^\pm X)}{\mathrm{d}\Omega \mathrm{d}z_1 \mathrm{d}z_2} \propto \frac{5}{9} D^{\mathrm{fav}}(z_1)\overline{D}^{\mathrm{dis}}(z_2) + \frac{5}{9} D^{\mathrm{dis}}(z_1)\overline{D}^{\mathrm{fav}}(z_2) + \frac{2}{9} D^{\mathrm{dis}}(z_1)\overline{D}^{\mathrm{dis}}(z_2)$$

$$N^C(\phi) = \frac{\mathrm{d}\sigma(e^+e^- \to \pi\pi X)}{\mathrm{d}\Omega \mathrm{d}z_1 \mathrm{d}z_2} = N^U(\phi) + N^L(\phi) \propto \frac{5}{9}[D^{\mathrm{fav}}(z_1) + D^{\mathrm{dis}}(z_1)][\overline{D}^{\mathrm{fav}}(z_2) + \overline{D}^{\mathrm{dis}}(z_2)] + \frac{4}{9} D^{\mathrm{dis}}(z_1)\overline{D}^{\mathrm{dis}}(z_2)$$

Flavor Tagging in Semi-Inclusive DIS

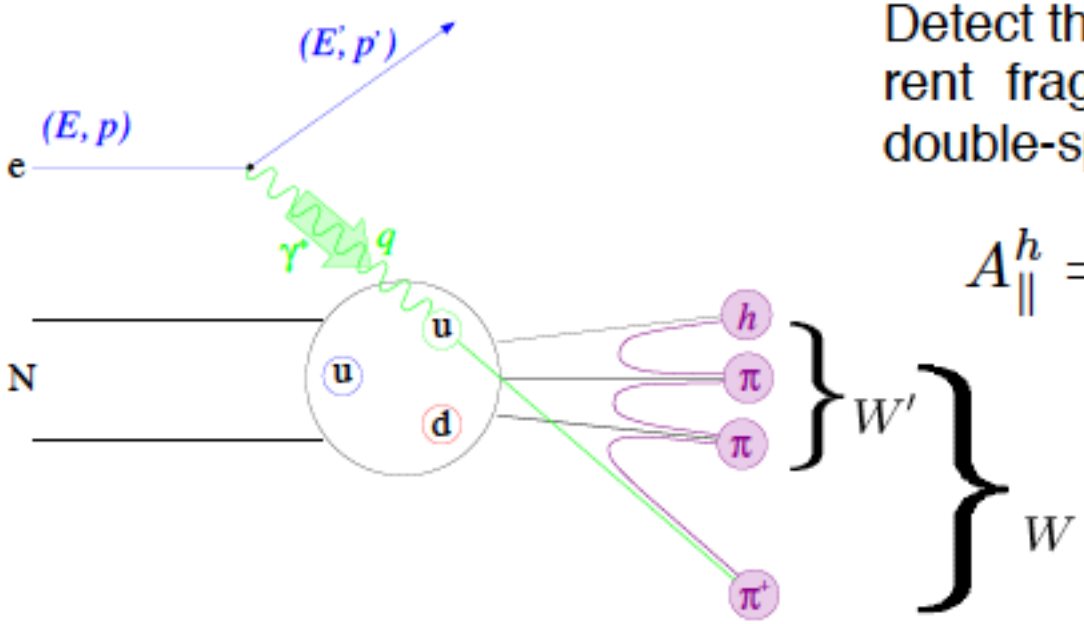

Detect the leading hadron from the current fragmentation and measure the double-spin asymmetry:

$$A_{\parallel}^{h} = f^{h} P_B P_T \cdot \mathcal{P}_{kin} \cdot A_{1N}^{h}$$

$$z = E_\pi / \nu$$

Assume leading order naive x-z separation:

$$A_{1N}^{h}(x, Q^2, z) \equiv \frac{\Delta\sigma^h(x, Q^2, z)}{\sigma^h(x, Q^2, z)} = \frac{\sum_f e_f^2 \Delta q_f(x, Q^2) \cdot D_f^h(z, Q^2)}{\sum_f e_f^2 q_f(x, Q^2) \cdot D_f^h(z, Q^2)}.$$

Each asymmetry measurement provides an independent constrain on Δq_f.

Semi-inclusive DIS at NLO

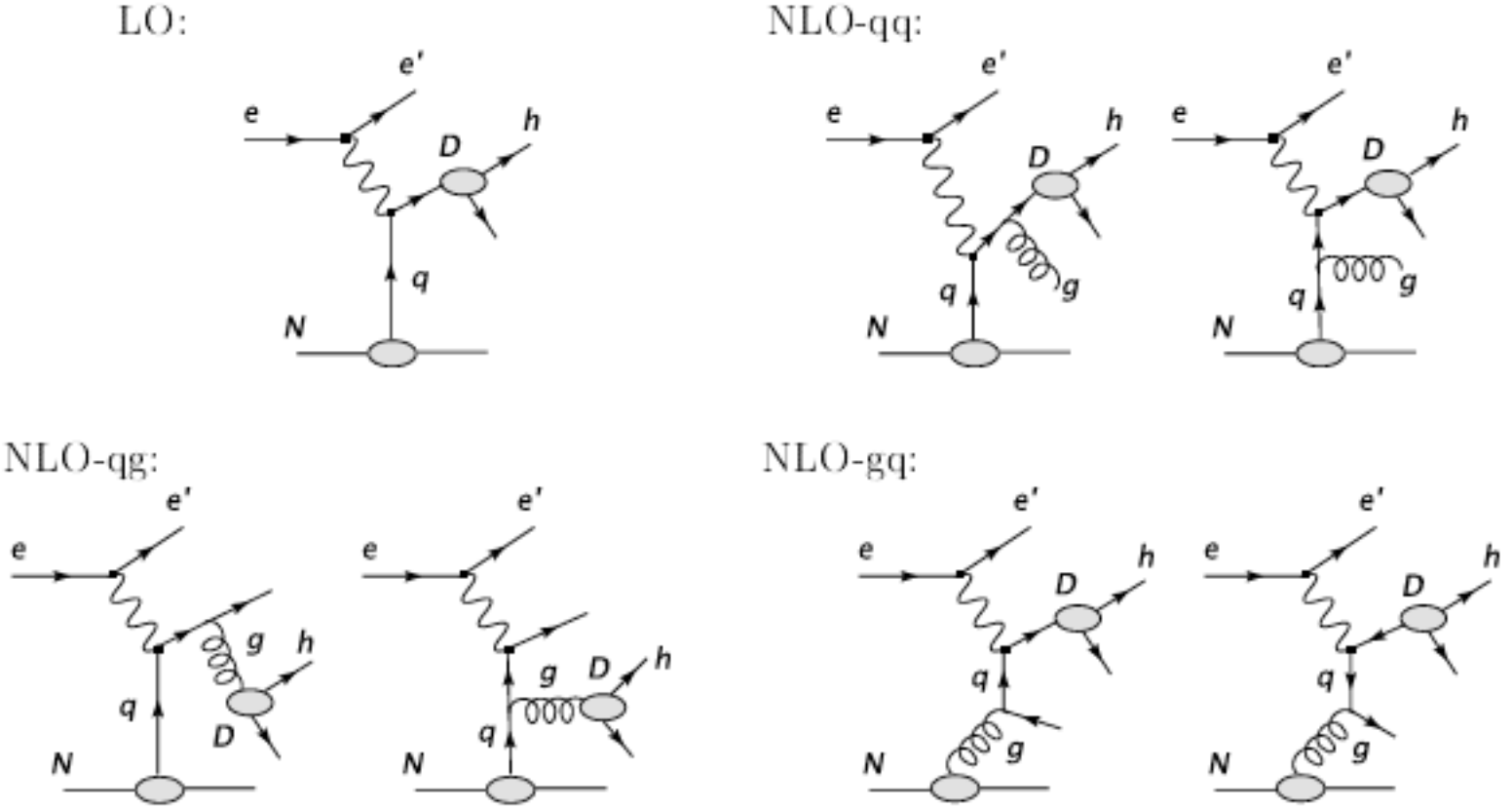

Figure 3: Semi-inclusive deep inelastic scattering diagrams at leading order (LO) and the next-to-leading order (NLO).

$$\sigma^h(x,z) = \sum_f e_f^2 q_f \left[1 + \otimes \frac{\alpha_s}{2\pi} C_{qq} \otimes\right] D_{q_f}^h + \left(\sum_f e_f^2 q_f\right) \otimes \frac{\alpha_s}{2\pi} C_{qg} \otimes D_G^h + G \otimes \frac{\alpha_s}{2\pi} C_{gq} \otimes \left(\sum_f e_f^2 D_{q_f}^h\right),$$

SIDIS Cross Section at the Next-to-Leading-Order

$$q(x,Q^2)\cdot D(z,Q^2)\Rightarrow \int\frac{dx'}{x'}\int\frac{dz'}{z'}q\left(\frac{x}{x'}\right)C(x',z')D\left(\frac{z}{z'}\right)=q\otimes C\otimes D$$

C are well-known Wilson coefficients (D. Graudenz, NPB432, 351(1994)).

$$\begin{aligned}\Delta\sigma^h &= \sum_i e_i^2\Delta q_i\left[1+\otimes\frac{\alpha_s}{2\pi}\Delta C_{qq}\otimes\right]D_{q_i}^h\\ &+ \left(\sum_i e_i^2\Delta q_i\right)\otimes\frac{\alpha_s}{2\pi}\Delta C_{qg}\otimes D_G^h+\Delta G\otimes\frac{\alpha_s}{2\pi}\Delta C_{gq}\otimes\left(\sum_i e_i^2 D_{q_i}^h\right)\end{aligned}$$

Isospin symmetry and charge conjugation: $D_G^h=D_G^{\bar{h}}$, $\sum_i e_i^2 D_{q_i}^h=\sum_i e_i^2 D_{q_i}^{\bar{h}}$.

- C and ΔC are very similar, NLO effects could cancel out in $A_{1N}^{\pi^++\pi^-}$.
- NLO global QCD-fit with inclusive and SIDIS data constrain Δq and ΔG.

BELLE

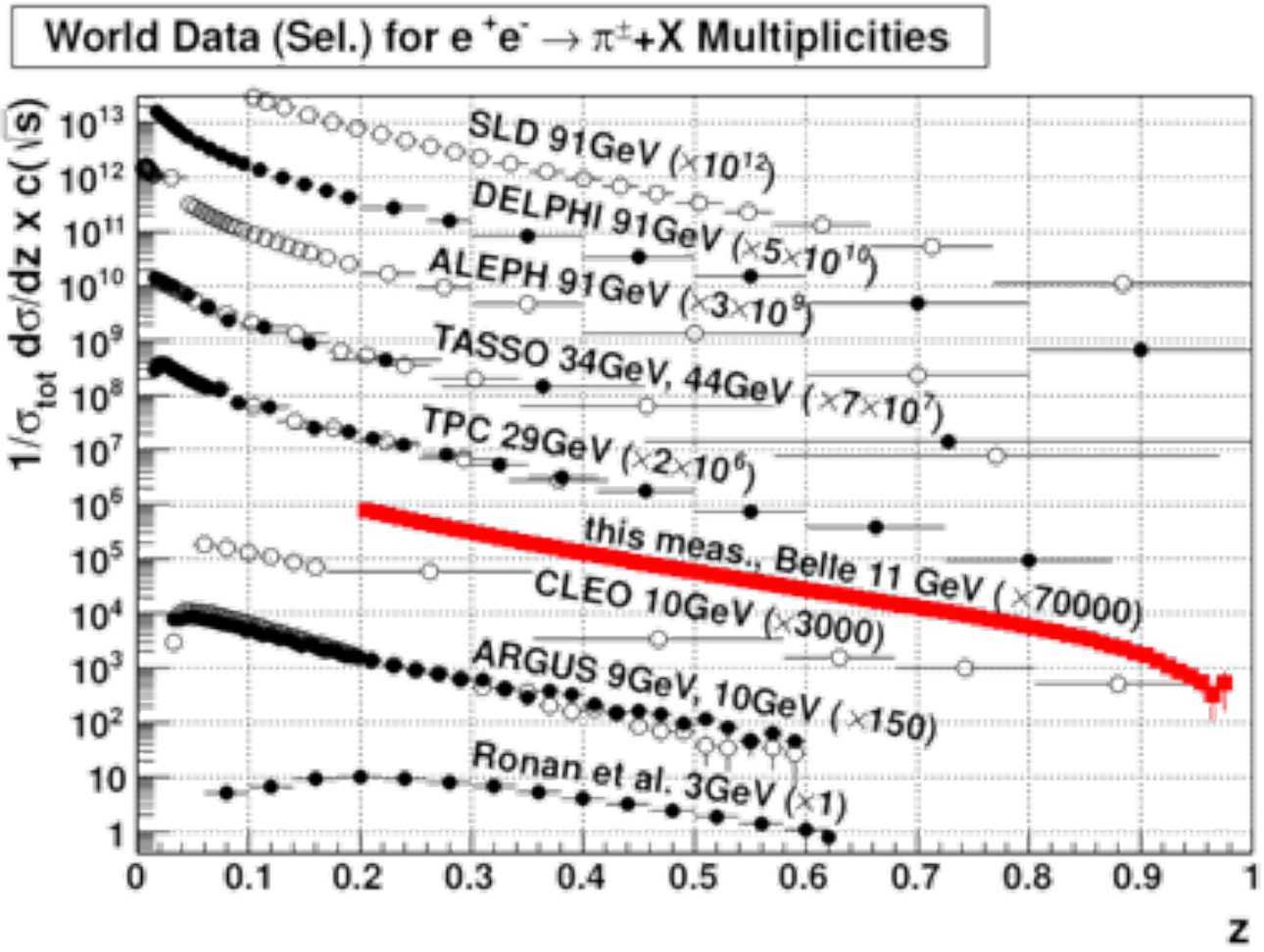
World Data (Sel.) for e⁺e⁻ → π±+X Multiplicities
1/σtot dσ/dz x c(√s)
SLD 91GeV (×10¹²)
DELPHI 91GeV (×5×10¹⁰)
ALEPH 91GeV (×3×10⁹)
TASSO 34GeV, 44GeV (×7×10⁷)
TPC 29GeV (×2×10⁶)
this meas., Belle 11 GeV (×70000)
CLEO 10GeV (×3000)
ARGUS 9GeV, 10GeV (×150)
Ronan et al. 3GeV (×1)
z

Belle results vs. World Data Selection

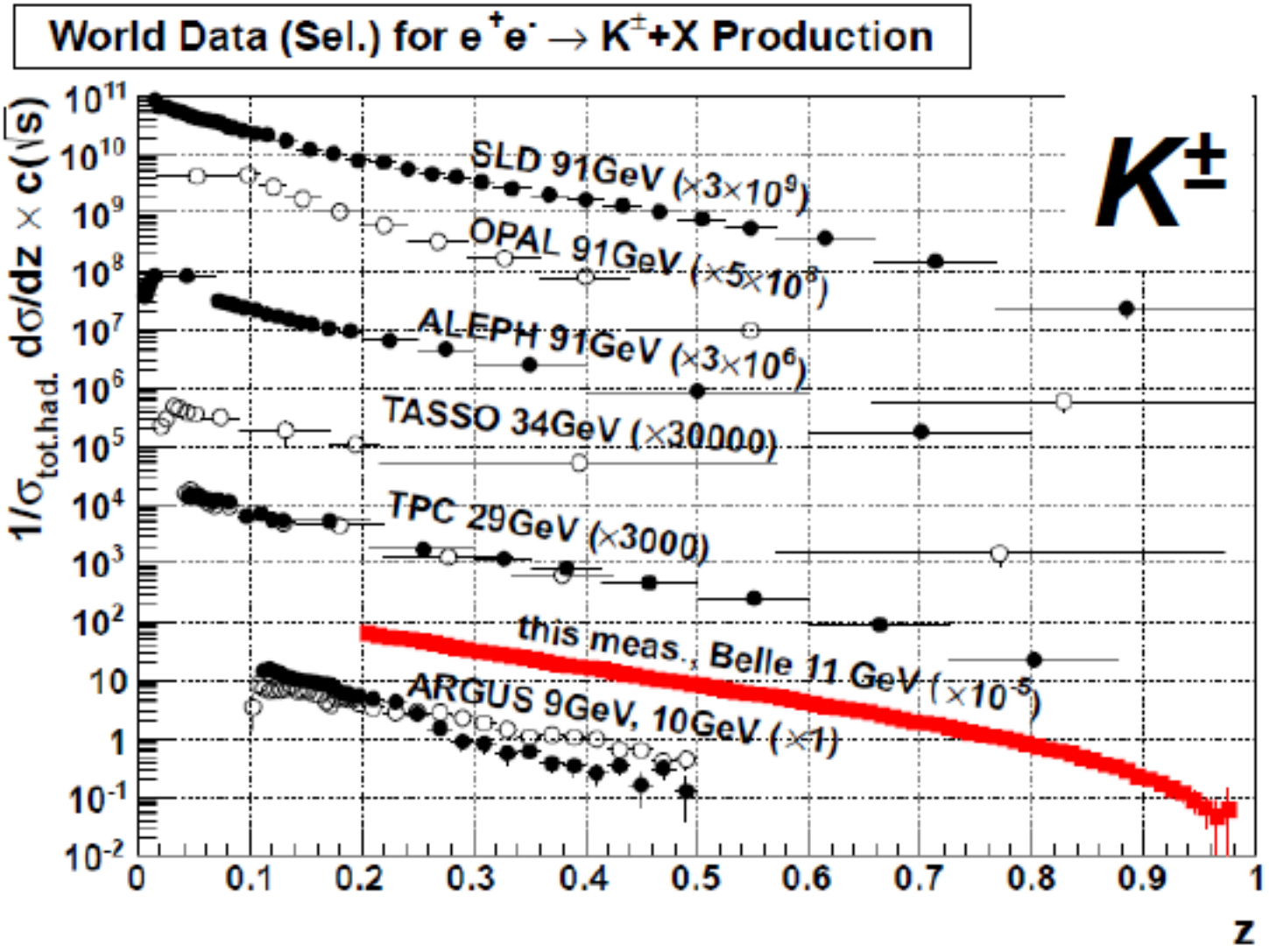

SIDIS HERMS Charged Hadron Multiplicities on a Proton Target

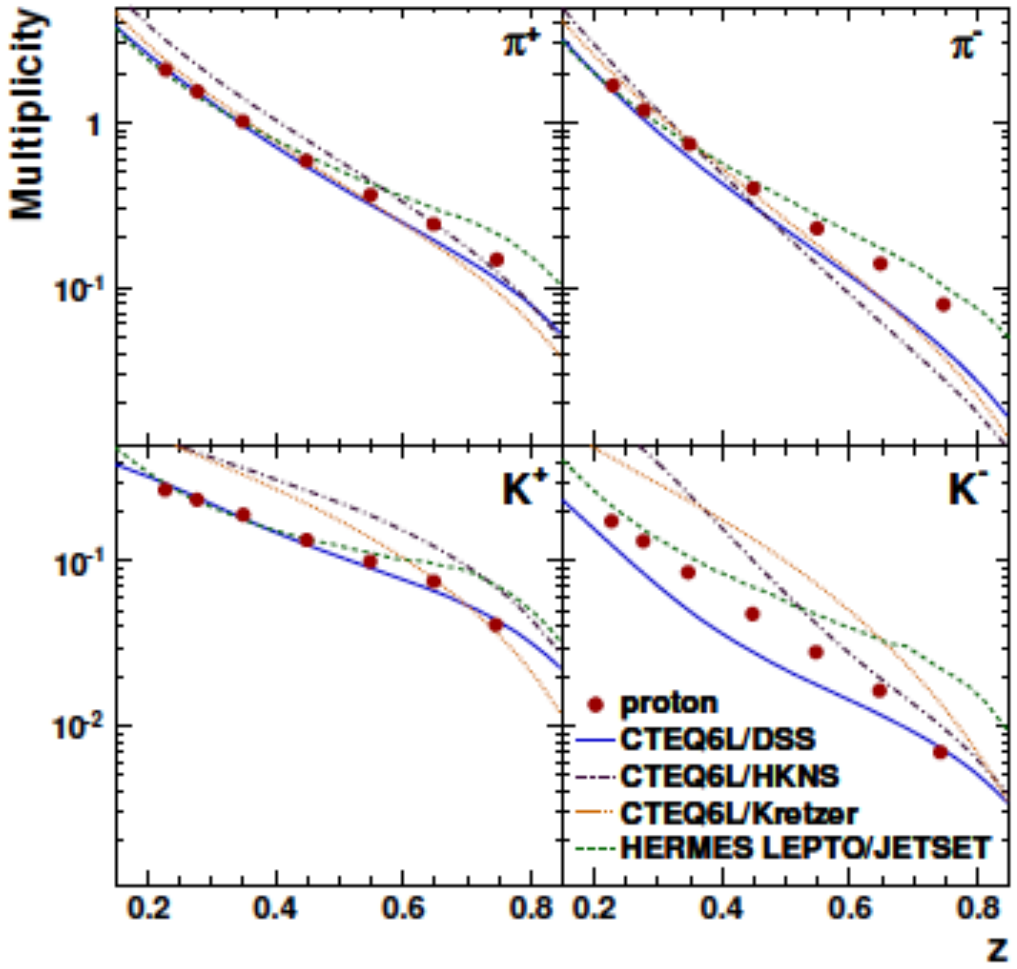

FIG. 9. Comparison of the vector-meson-corrected multiplicities measured on the proton for various hadrons with LO calculations using CTEQ6L parton distributions [45] and three compilations (see text) of fragmentation functions. Also shown are the values obtained from the HERMES Lund Monte Carlo. The statistical error bars on the experimental points are too small to be visible.

SIDIS COMPASS Charged Hadron Multiplicities on a Proton Target

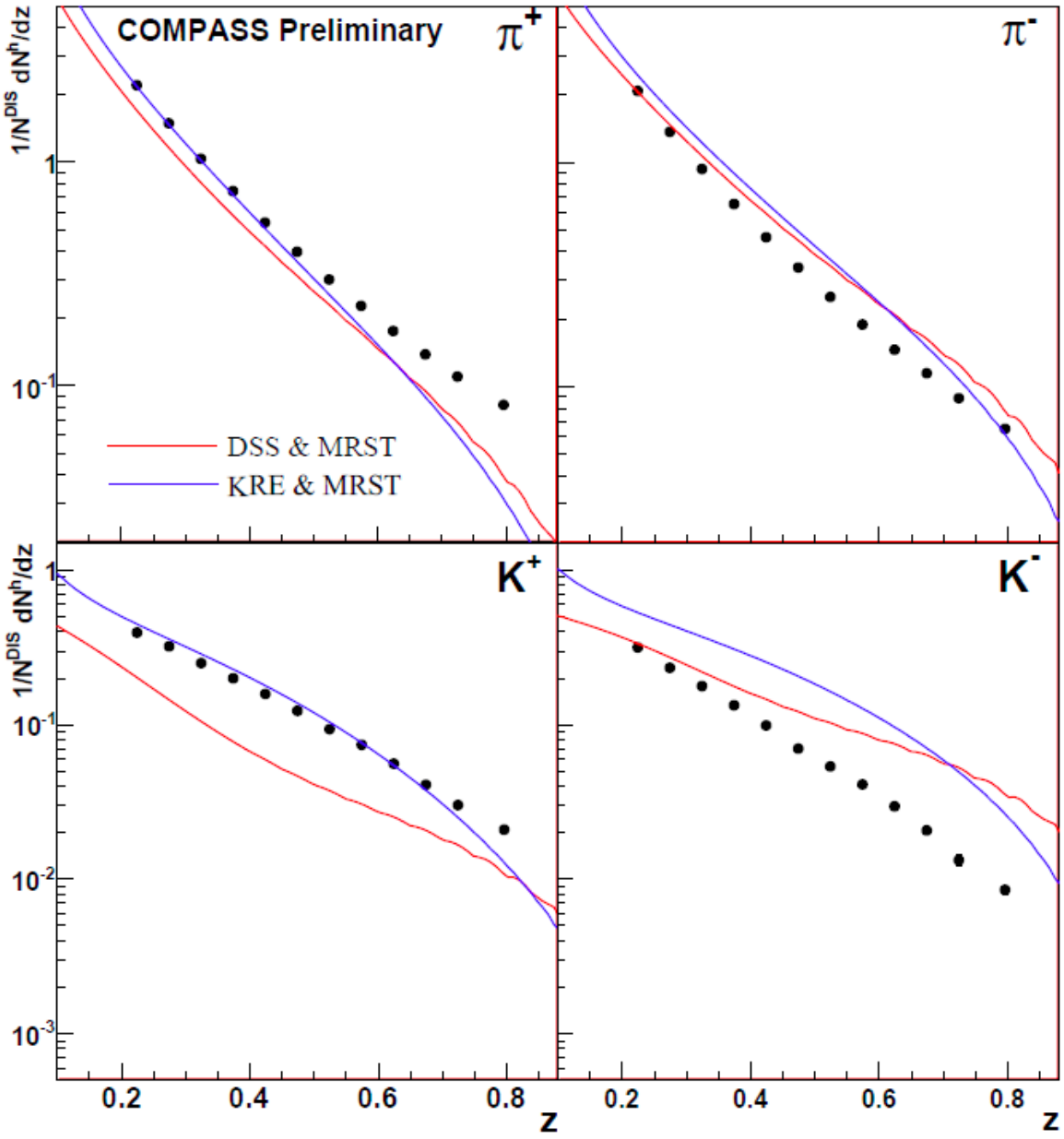

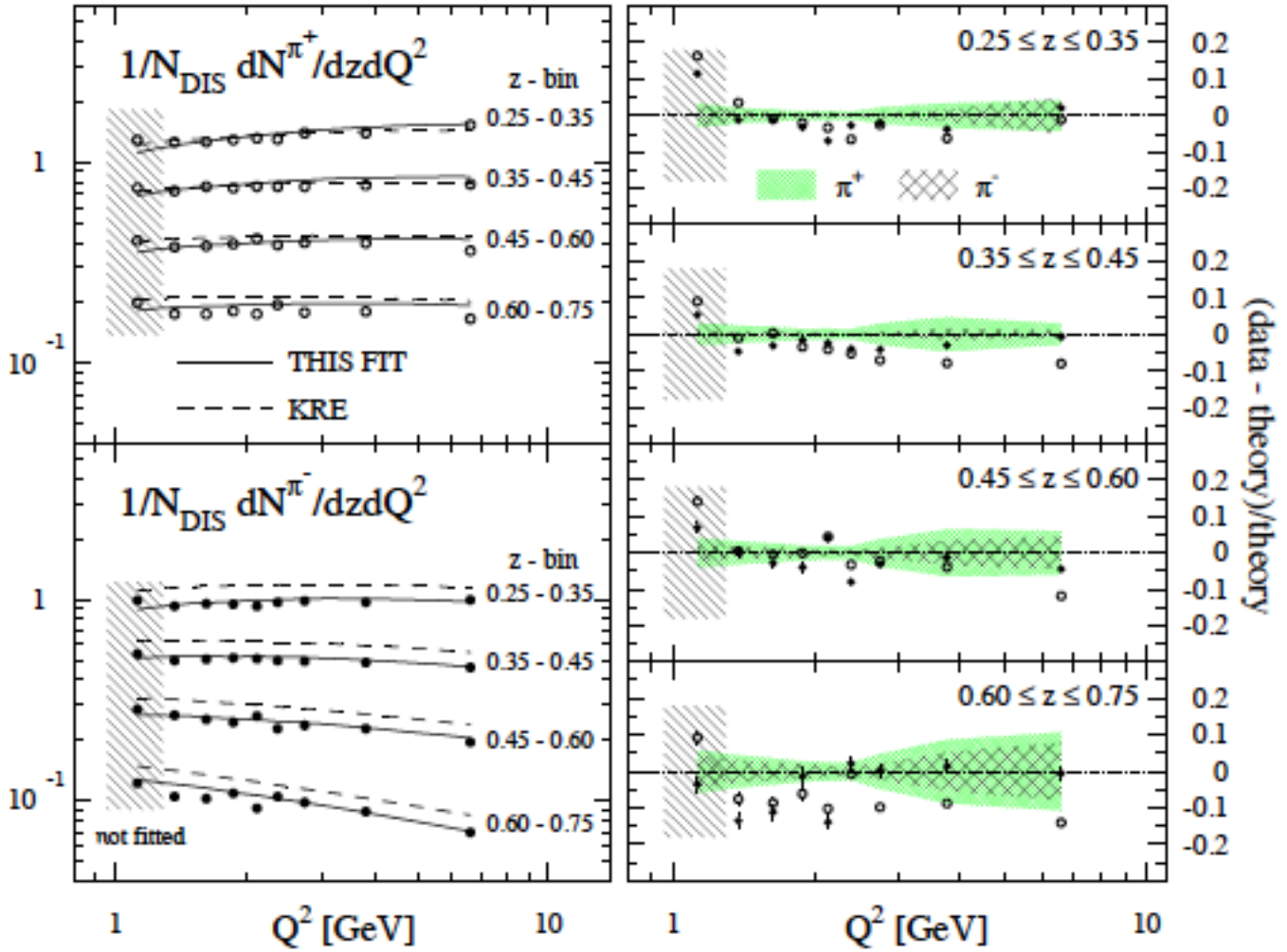

FIG. 4: **L.h.s.** comparison of our NLO results for charged pion multiplicities in SIDIS, $(1/N_{DIS})dN^{\pi^\pm}/dzdQ^2$, with preliminary HERMES data [18]. Also shown are the results obtained with the KRE [7] parametrization. **R.h.s.** "(data-theory)/theory" for our NLO results, open and full circles denote π^+ and π^- multiplicities, respectively. The shaded bands indicate estimates of theoretical uncertainties due to finite bin-size effects (see text).

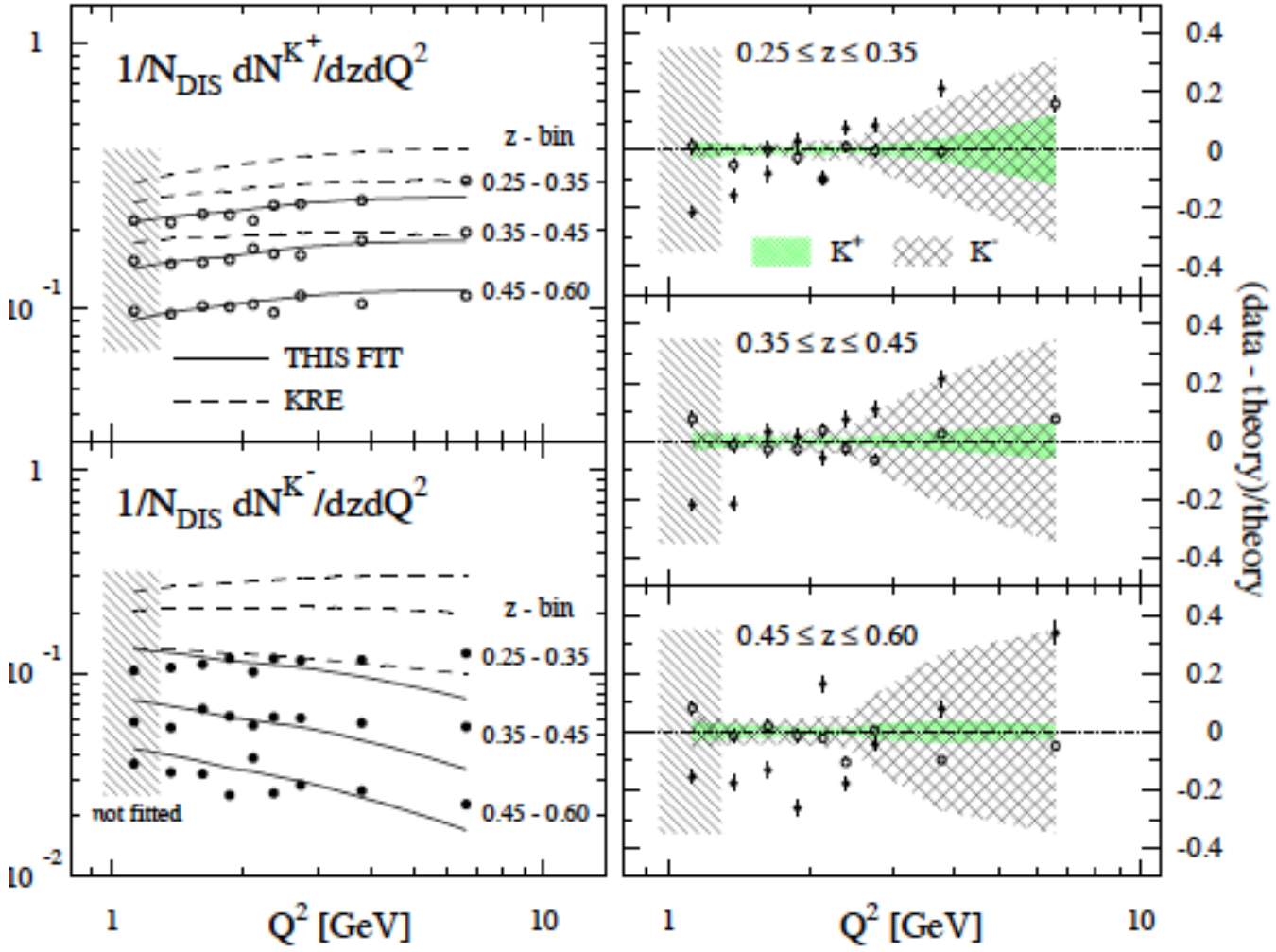

FIG. 13: Same as in Fig. 4 but now for charged kaons.

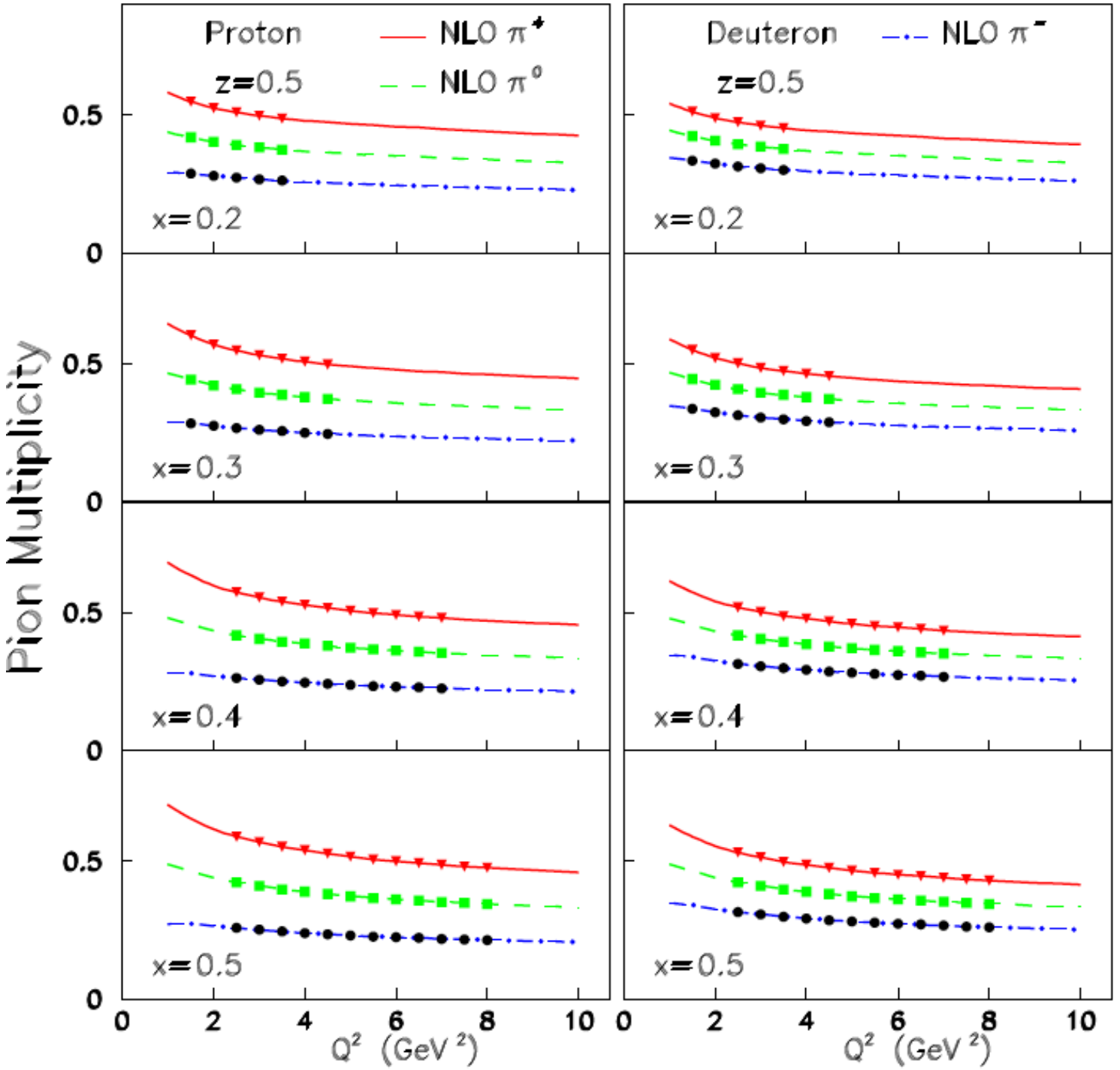

Projected precision of JLab-12 GeV sidis measurements

Spin dependent frag. Func.

to access quark transversity distributions …

- Transversity distribution is chiral--odd, not accessible through inclusive deep-inelastic scattering. Need to be combined with another chiral-odd object, i.e. Collins fragmentation function.

Through target single spin asymmetry in **semi-inclusive DIS**.

J.C. Collins, NPB 396, 161(1993).

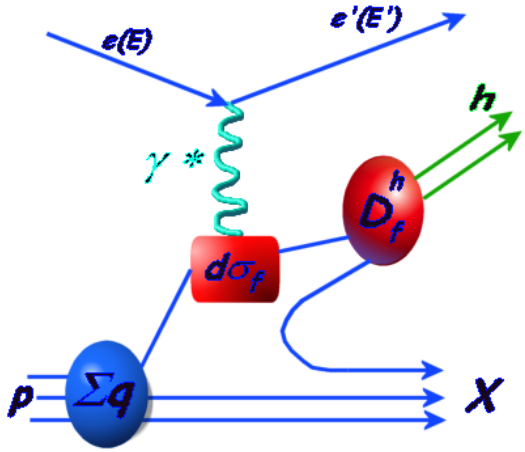

$$A_{UT}^{Collins}(x,z) \propto \frac{\sum_q e_q^2\, \delta q(x) \otimes H_{1q}^{\perp h}(z, P_{h\perp}^2)}{\sum_q e_q^2\, q(x) \otimes D_{1q}^h(z, P_{h\perp}^2)}$$

Collins frag. fun. can be accessed in e^+e^- collisions (BELLE experiment at KEK).

Collins-Soper Frame

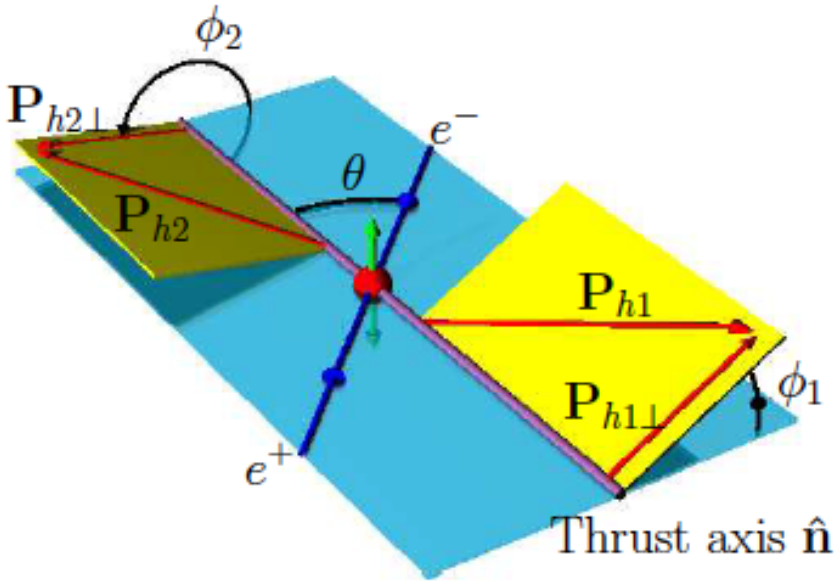

FIG. 1: Definition of the azimuthal angles of the two hadrons. In each case, ϕ_i is the angle between the plane spanned by the lepton momenta and the thrust axis $\hat{n}$, and the plane spanned by $\hat{n}$ and the hadron transverse momentum $P_{hi\perp}$.

$$A_{12} \propto \cos(\phi_1 + \phi_2) \frac{H_1^{\perp,[1]} \bar{H}_1^{\perp,[1]}}{D_1^{[0]} \bar{D}_1^{[0]}}$$

Gottfried-Jackson Frame

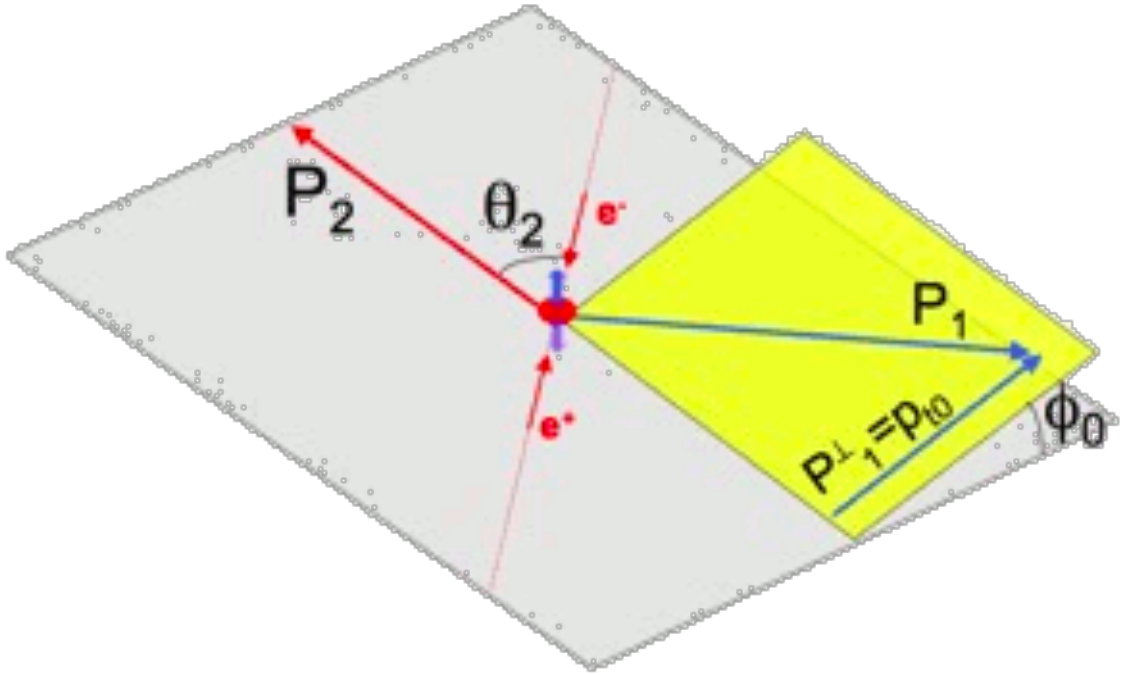

$$A_0 \propto \cos(2\phi_0) \frac{\mathcal{F}[\mathcal{W} H_1^\perp \bar{H}_1^\perp]}{\mathcal{F}[D_1 \bar{D}_1]}$$

BELLE

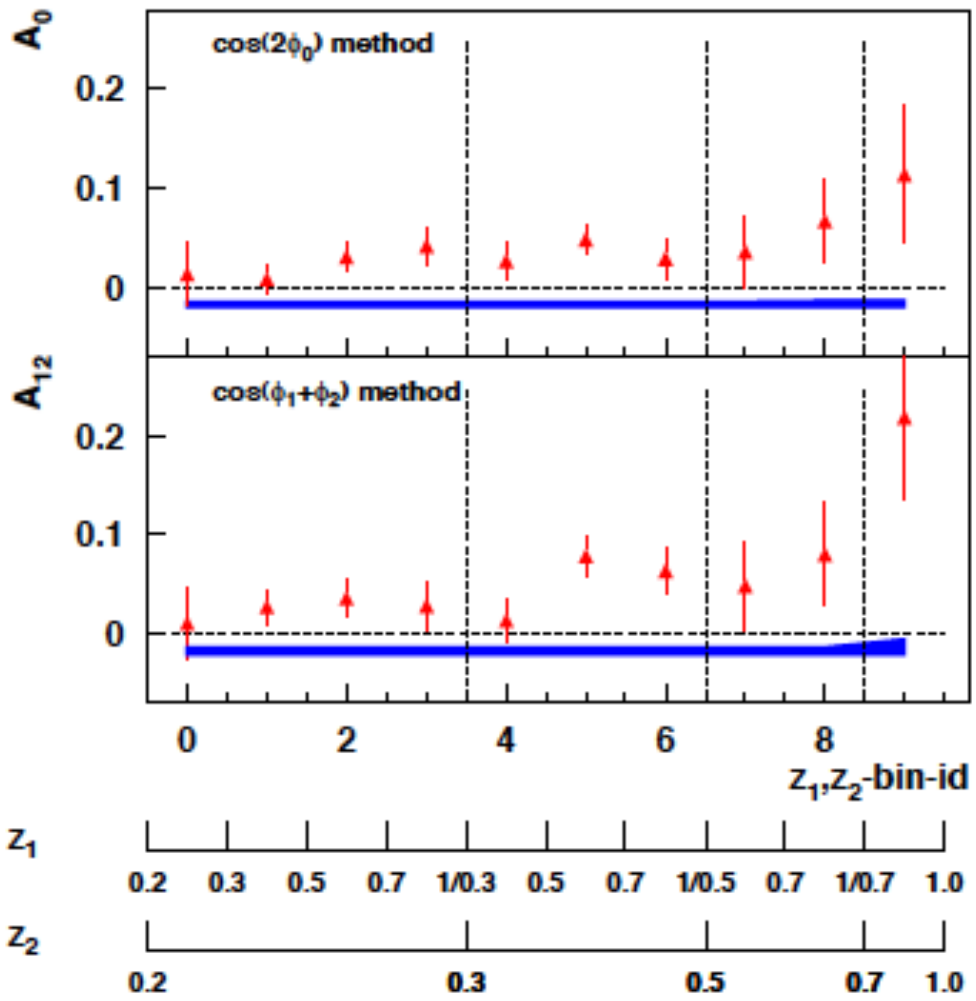

FIG. 3: Values of A_0 and A_{12} as functions of z, corrected for the contribution of charm events. The lower scales show the boundaries of the bins in z_1 and z_2; see the text. The shaded band shows the size of the systematic errors.

BARBAR

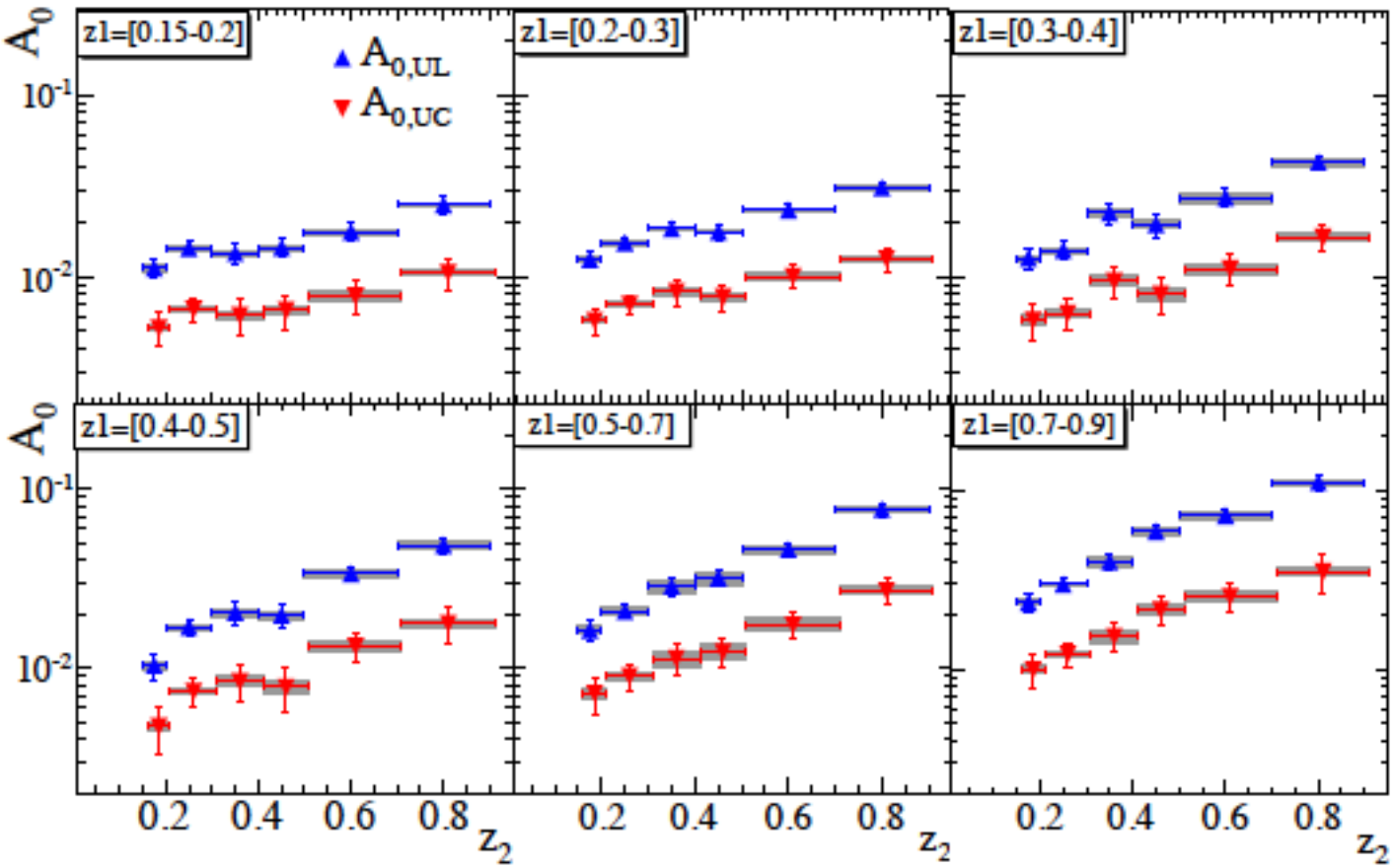

FIG. 15: (color online). Collins asymmetries for light quarks measured in bins of fractional energies (z_1, z_2), in RF0. Asymmetries for the UL (up triangles) and UC (down triangles) ratios are reported, with statistical error bars and systematic uncertainties represented by the bands around the points.

STAR 2006 Preliminary p+p -> hadron azimuthal distribution

Midrapidity Collins: A_N is related to $\Delta_T f(x) \otimes \Delta D(z)$

Measure an azimuthal modulation of a π in a jet

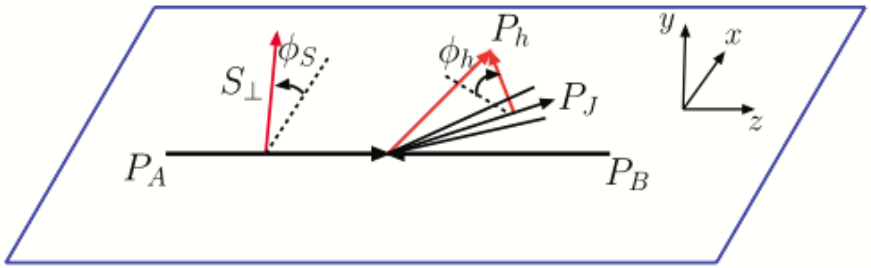

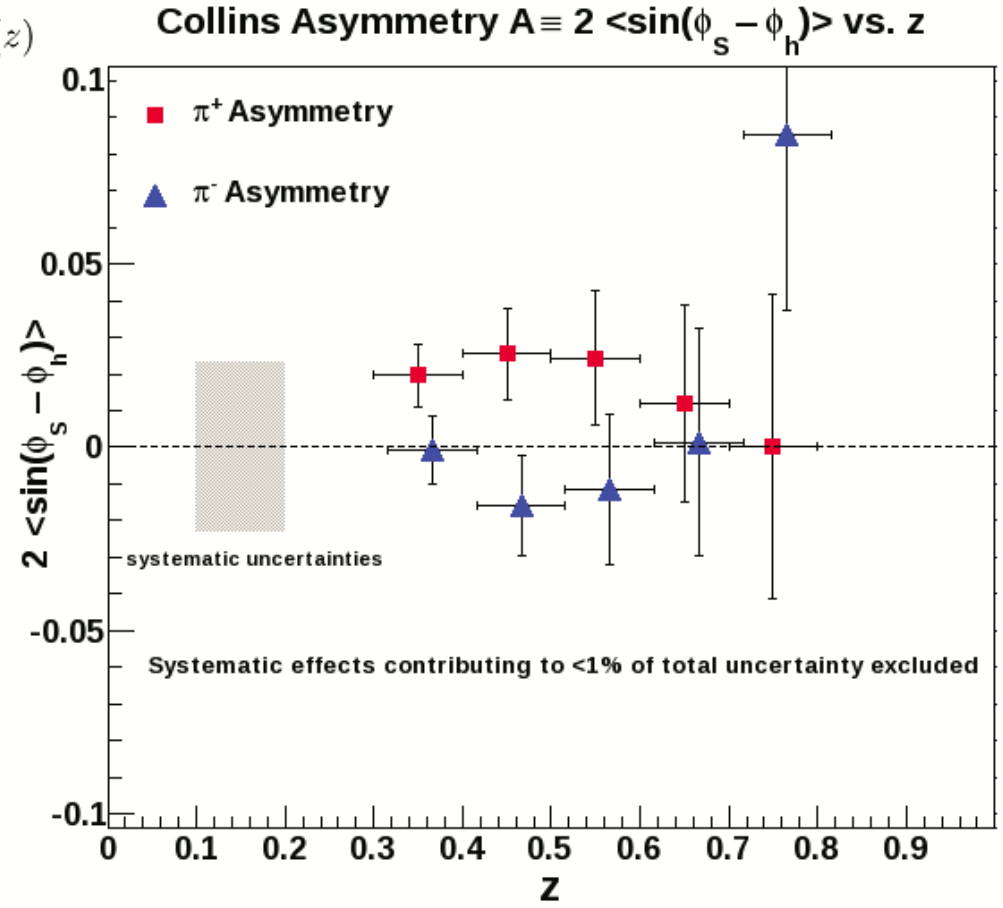

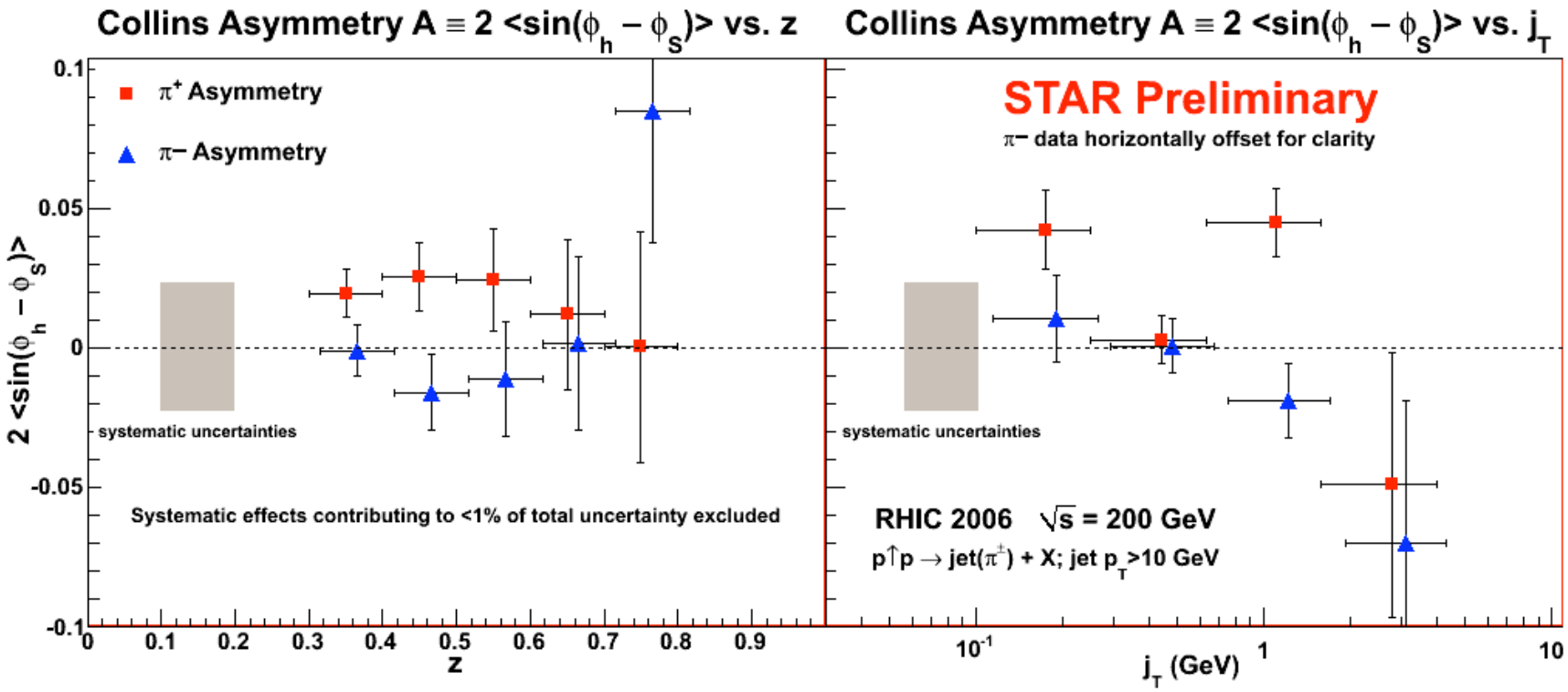
Collins Asymmetry A ≡ 2 <sin(φh − φS)> vs. z
Collins Asymmetry A ≡ 2 <sin(φh − φS)> vs. jT
π+ Asymmetry
π− Asymmetry
systematic uncertainties
Systematic effects contributing to <1% of total uncertainty excluded
2 <sin(φh − φS)>
z
STAR Preliminary
π− data horizontally offset for clarity
systematic uncertainties
RHIC 2006 √s = 200 GeV
p↑p → jet(π±) + X; jet pT>10 GeV
jT (GeV)

Di-hadron Correlation

- -> measure simultaneous **azimuthal modulation** of **two pion pair yields** in **opposing hemispheres**

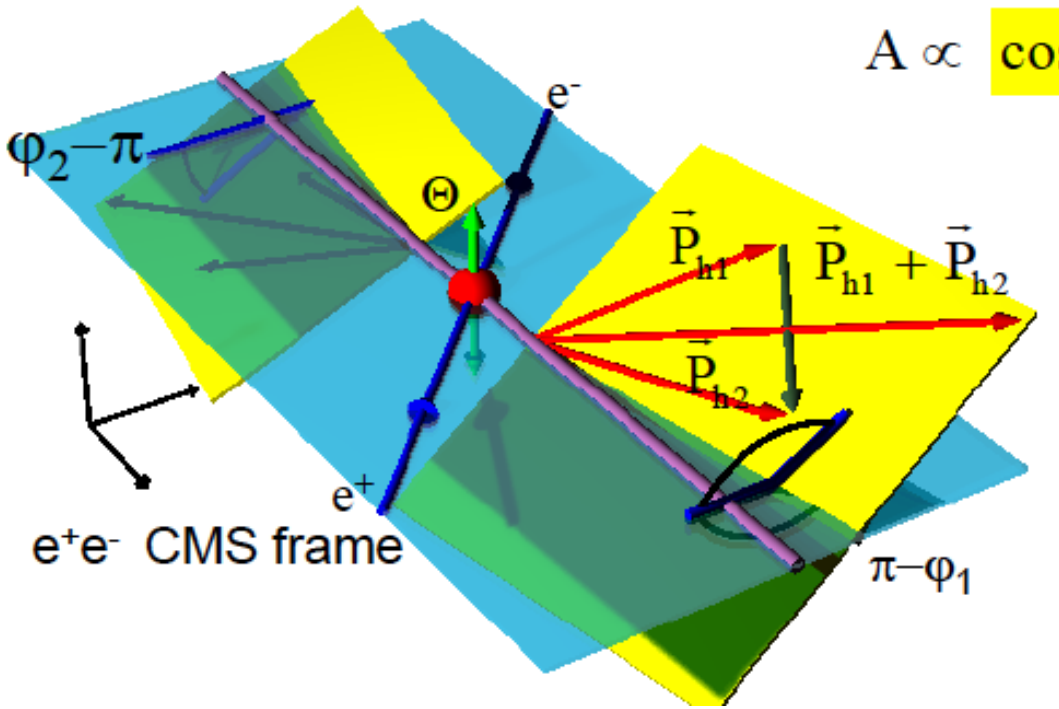

$$A \propto \cos(\varphi_1+\varphi_2)\, H_1^{\sphericalangle}(z_1,m_1)\overline{H}_1^{\sphericalangle}(z_2,m_2)$$

- Transverse quark spin distributions **δq** can be extracted from measurements in **pp** and **SIDIS experiments** via:

  - **transversity** x **Collins FF:** $\delta q \times H_1^{\perp}$

  - **transversity** x **Interference FF (IFF):** $\delta q \times H_1^{\sphericalangle}$

STAR $\pi^+\pi^-$ **IFF**

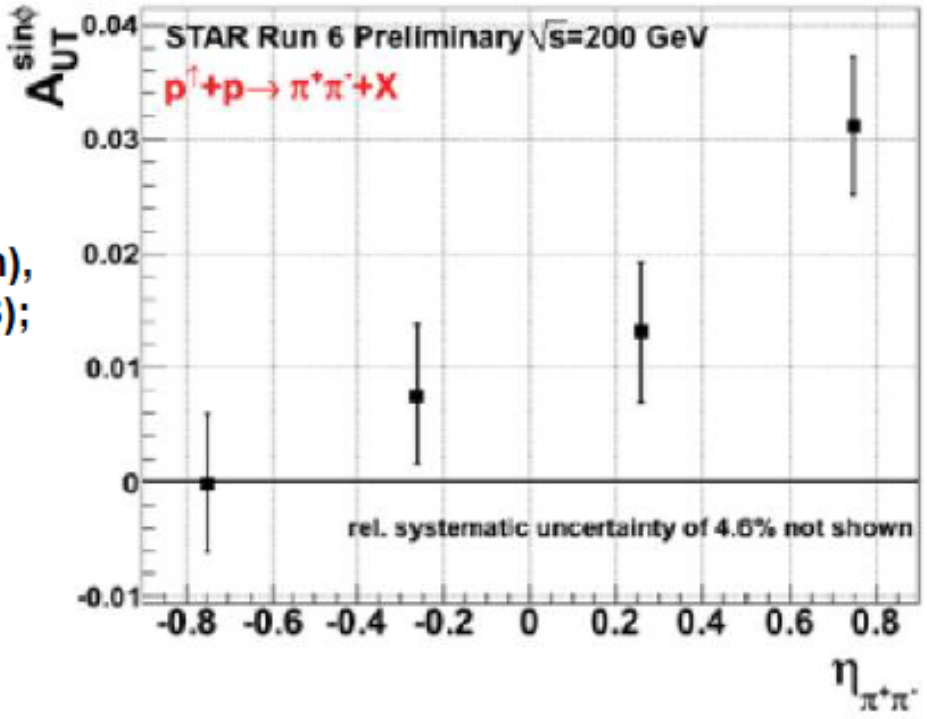

G. Igo et al (STAR collaboration), AIP Conf. Proc. 1523, 188 (2013);

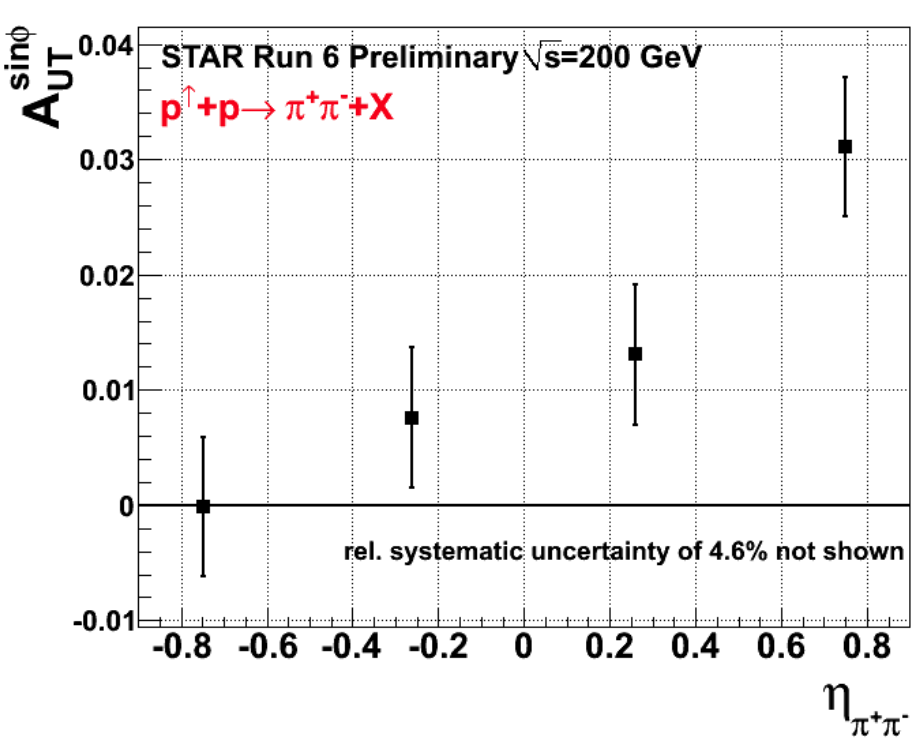
STAR Run 6 Preliminary √s=200 GeV
p↑+p→ π+π-+X
rel. systematic uncertainty of 4.6% not shown
A_UT^sinφ
η_π+π-

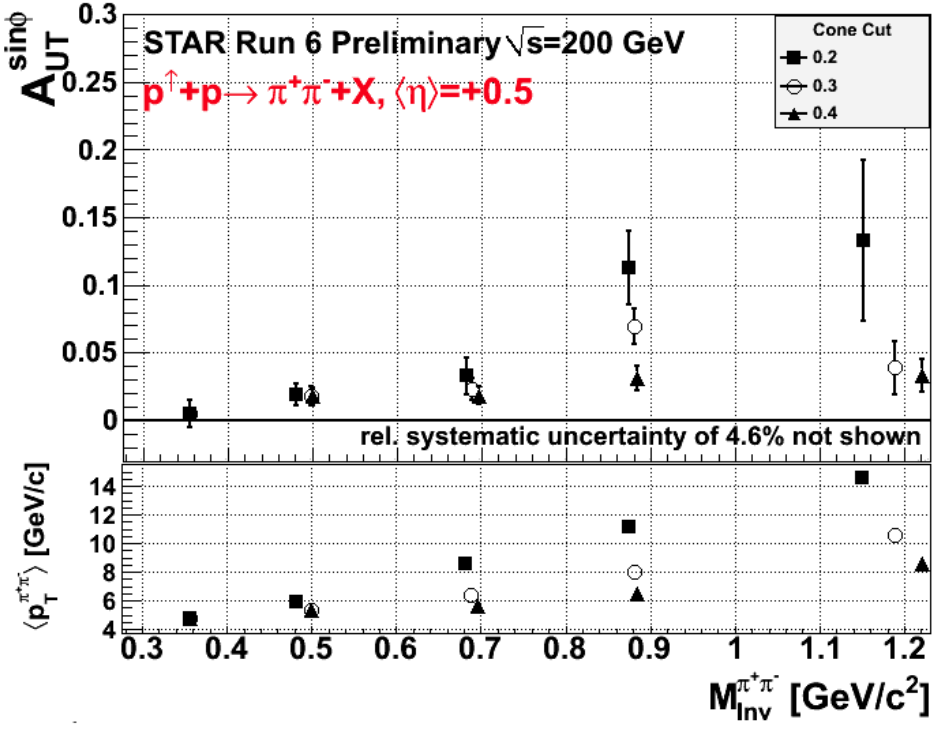
STAR Run 6 Preliminary √s=200 GeV
p↑+p→ π+π-+X, ⟨η⟩=+0.5
Cone Cut
0.2
0.3
0.4
rel. systematic uncertainty of 4.6% not shown
A_UT^sinφ
⟨p_T^π+π-⟩ [GeV/c]
M_Inv^π+π- [GeV/c²]

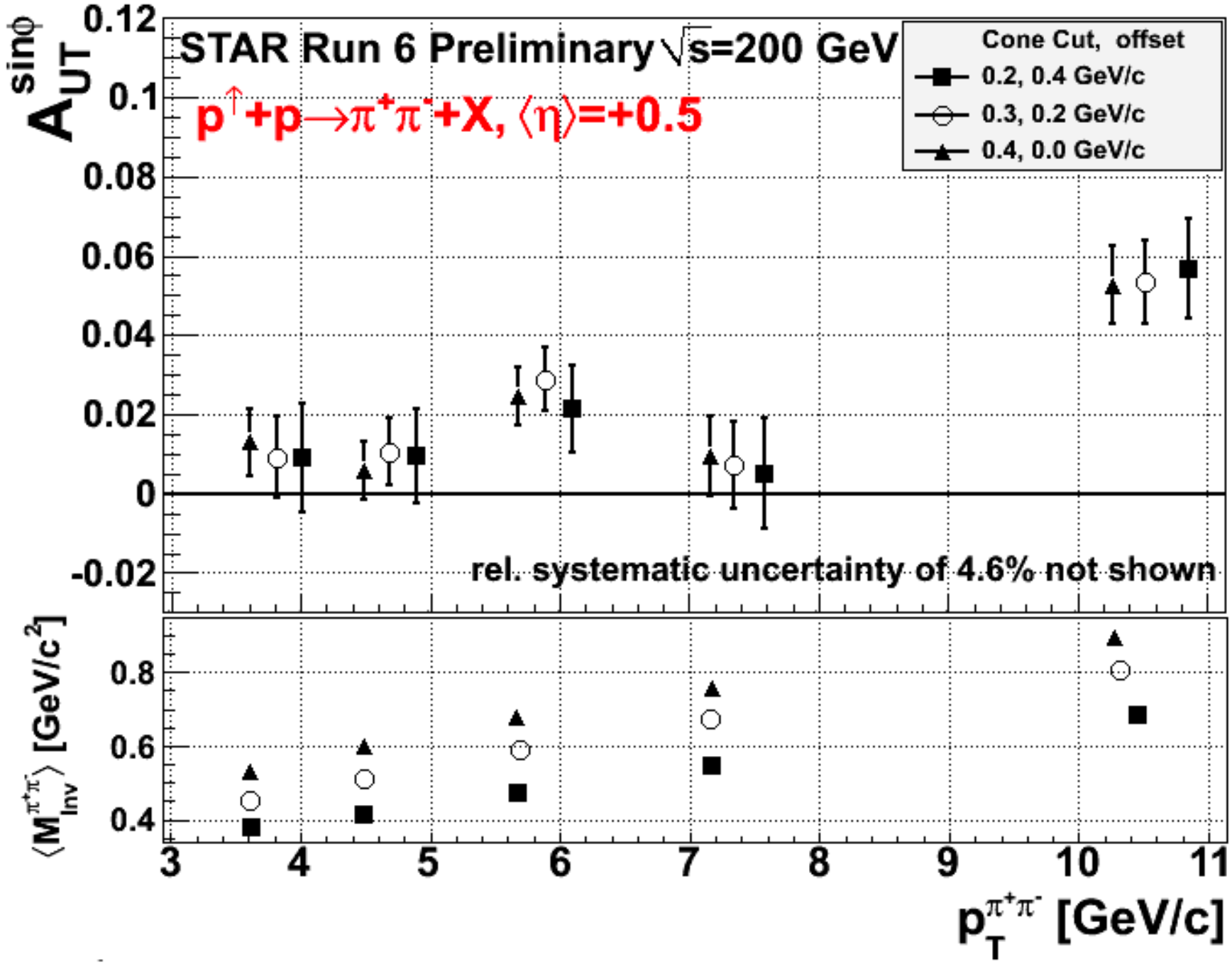
STAR Run 6 Preliminary √s=200 GeV
p↑+p→π+π-+X, ⟨η⟩=+0.5
Cone Cut, offset
0.2, 0.4 GeV/c
0.3, 0.2 GeV/c
0.4, 0.0 GeV/c
rel. systematic uncertainty of 4.6% not shown
A_UT^sinφ
⟨M_inv^π+π-⟩ [GeV/c²]
p_T^π+π- [GeV/c]

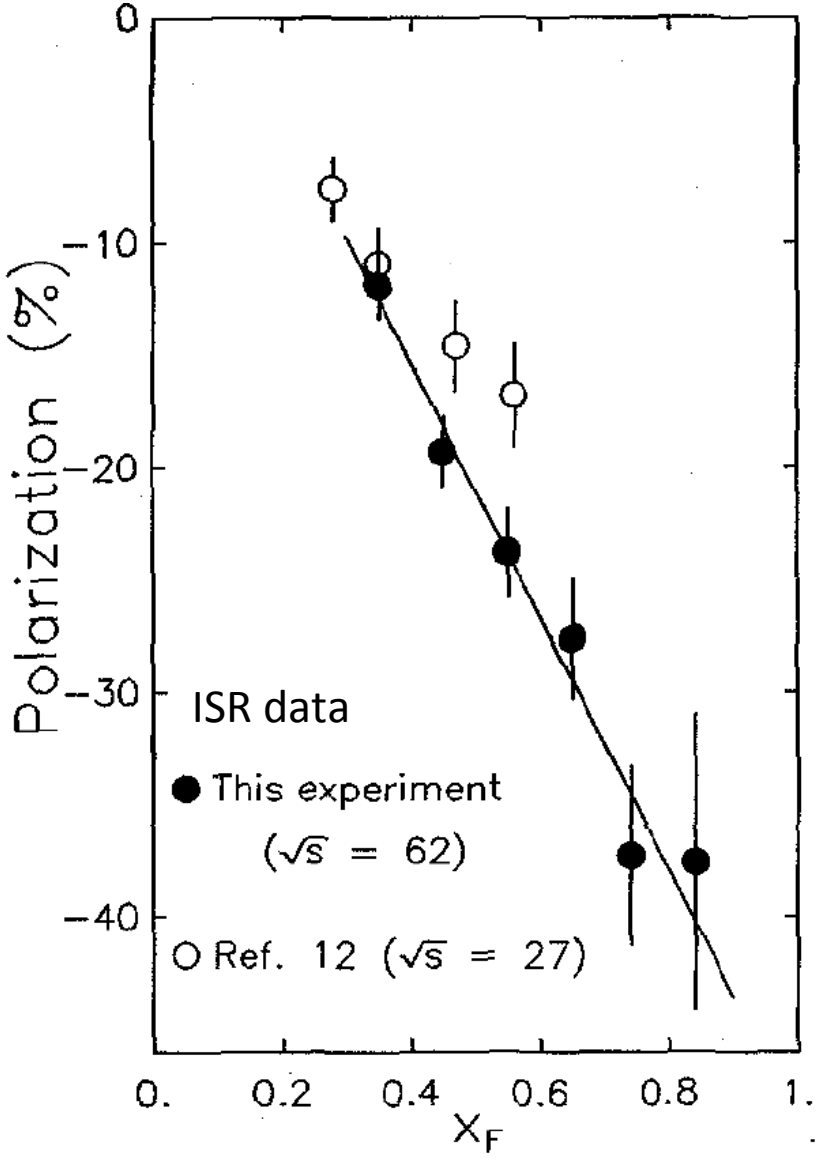

$$p + p \rightarrow \Lambda^{\uparrow} + X$$

The puzzle of large induced polarization of hyperon in p+p

Fig. 3. P_{Λ^0} versus x_F for those data in fig. 2 with $p_t > 0.96$ GeV/c (the average $p_t = 1.14$ GeV/c). The straight line is the fit discussed in the text. The open circles are Fermilab results from ref. [12] with $p_t > 0.95$ GeV/c.

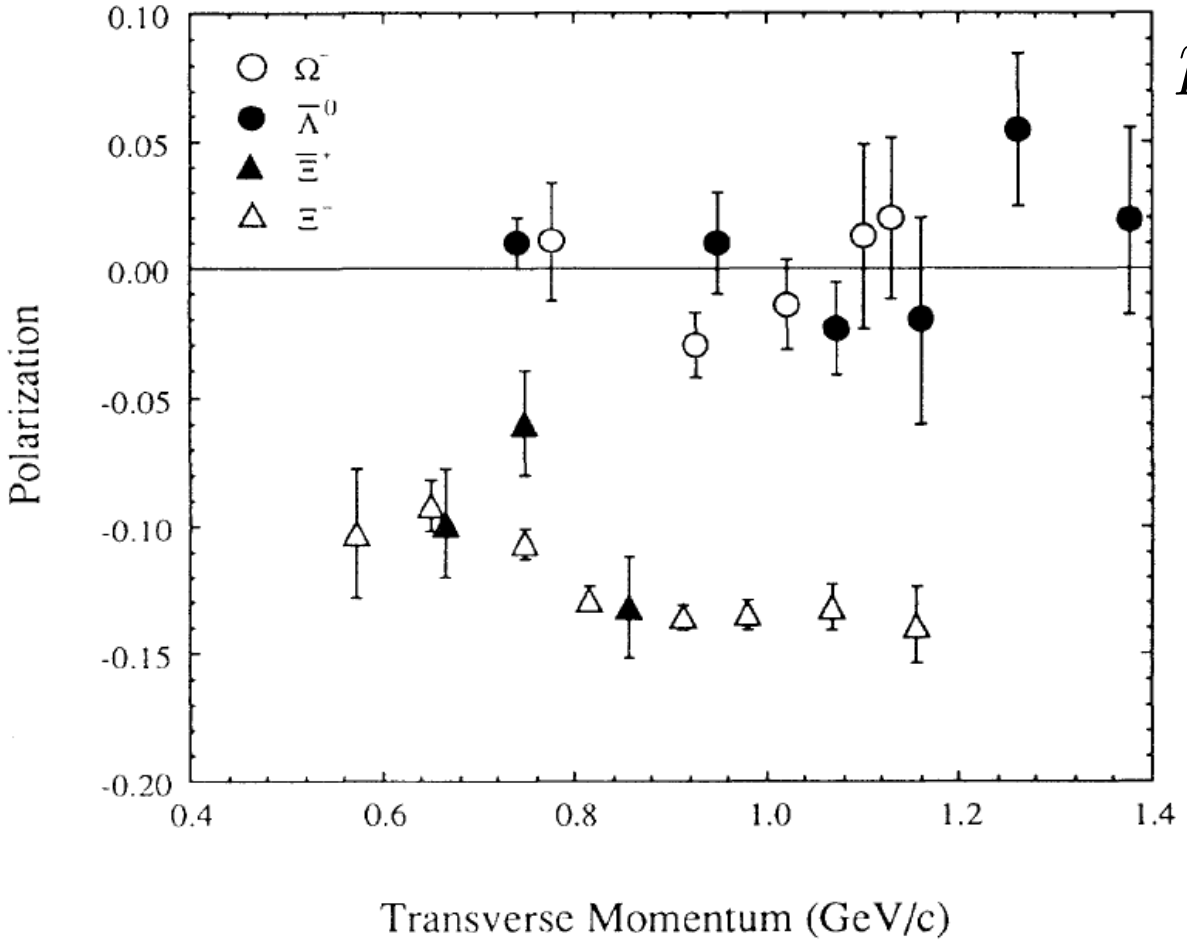

$$p + p \rightarrow H^{\uparrow} + X$$

Induced Hyperon Polarization

FIG. 3. Comparison of the Ω^- polarization with those of the $\bar{\Xi}^+$, $\bar{\Lambda}^0$, and Ξ^- as a function of the transverse momentum. For a given transverse momentum, the average x_F of the $\bar{\Lambda}^0$ is slightly lower than that of the Ω^-. The Ξ^- and $\bar{\Xi}^+$ data are from this experiment (see Refs. [4] and [10]), and the 400 GeV/c $\bar{\Lambda}^0$ results are taken from Ref. [8].

Left-Right Asymmetry of Lambda

E704. PRL 75, 3073(1995).

$$p^{\uparrow} + p \rightarrow \Lambda + X$$

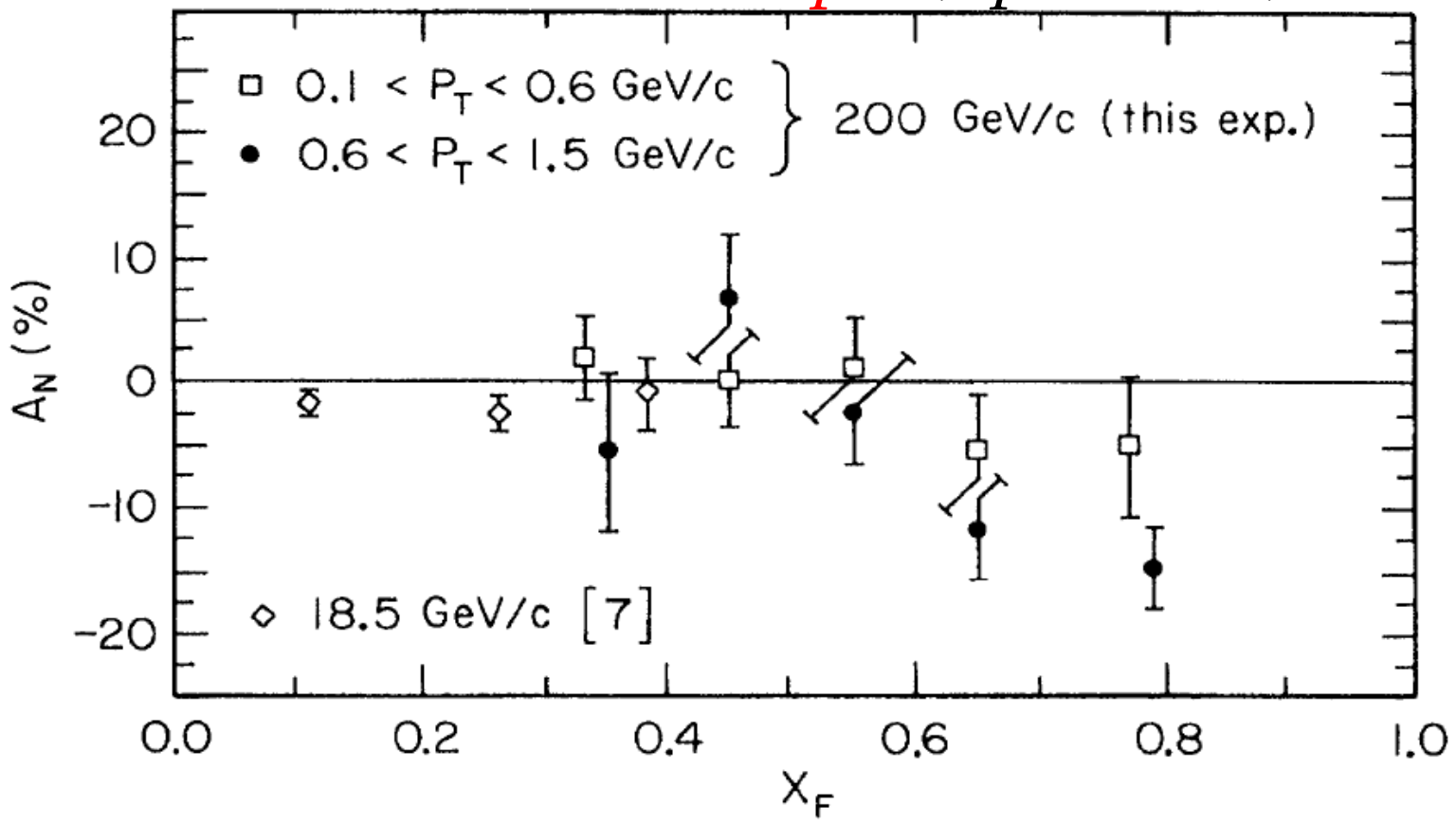

FIG. 3. A_N data for $p\uparrow + p \rightarrow \Lambda^0 + X$ as a function of x_F. Data at 18.5 GeV/c [7] ($\diamond$) are also shown.

D_{NN}: Transverse Spin Transfer to Lambda

$$p^{\uparrow} + p \rightarrow \Lambda^{\uparrow} + X$$

(transversity)*(final-spin dependent Frag. Func.)

E704: PRL 78, 4003 (1997)

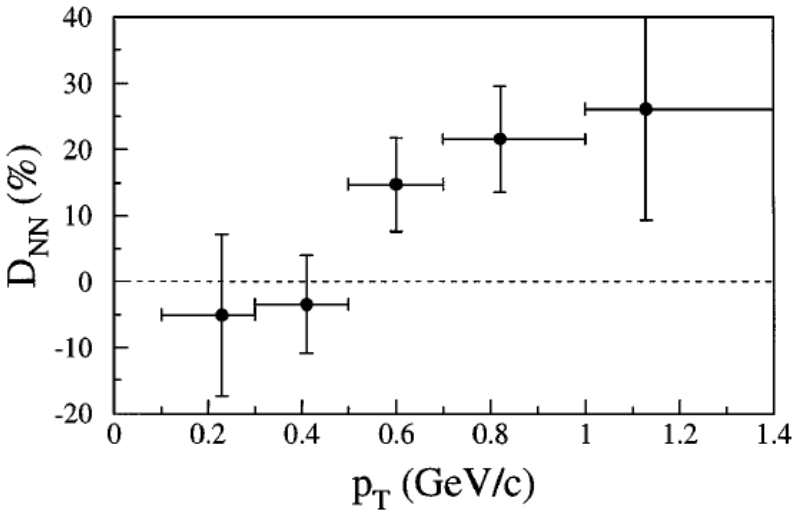

FIG. 1. Depolarization D_{NN} data as a function of p_T in $p\uparrow + p \rightarrow \Lambda^0 + X$ at 200 GeV/c. The errors shown are statistical only.

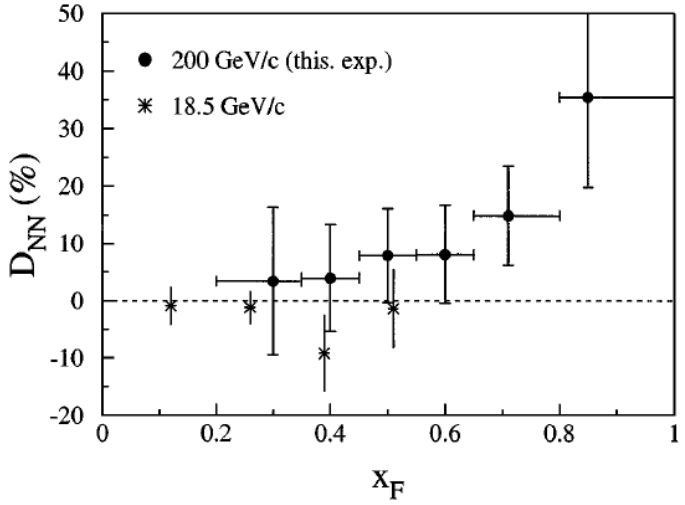

FIG. 2. Depolarization D_{NN} data as a function of x_F. The errors shown are statistical only. Also shown are D_{NN} measurements at 18.5 GeV/c from Ref. [12] ($\langle p_T \rangle \sim 1.0$ GeV/c for the plotted points).